SYNTHESIS AND CHARACTERIZATION OF HYBRID AMINOPROPYL SILANE-BASED COATINGS ON STAINLESS STEEL SUBSTRATES

S. M. Hanetho[a], I. Kaus[b], A. Bouzga[c], C. Simon[c], T. Grande[a] and M.-A. Einarsrud[1, *]

[a]Department of Materials Science and Engineering, Norwegian University of Science and Technology, 7491 Trondheim, Norway

[b]SINTEF Materials and Chemistry, 7465 Trondheim, Norway

[c]SINTEF Materials and Chemistry, 0314 Oslo, Norway

Abstract

Transparent and homogeneous hybrid aminopropyl silane-based coatings on steel were prepared by the sol-gel method using hydrolyzed γ-APS as a precursor. The coatings were fabricated by dip coating, and the effect of pH, water/silane ratio and solvent/silane ratio during the coating process was investigated with respect to thermal stability, coating thickness, roughness, contact angle and abrasion resistance. The thickness of the coatings was controlled by the preparation conditions as well as the viscosity of the sols and varied between 0.17 and 4.1 μm. The coatings were in general smooth and the roughness in the order of a few nm. The coatings possessed hydrophilic character with contact angles of water from 65 to 80 °, while organic pentadecane wetted the coatings. The abrasion resistance improved with decreasing pH of the water used during hydrolysis of the silane. The abrasion resistant properties of the coatings were characterized with respect to delamination and smearing. Thicker coatings were delaminated while thinner coatings were smeared and displayed lubricating properties. The coatings were thermally stable up to 350 °C, and also displayed a low pore volume and a low surface area.

* Author to whom correspondence should be addressed. e-mail: mari-ann.einarsrud@material.ntnu.no

1. Introduction

Hybrid inorganic-organic materials combine the advantages of the flexibility and good impact resistance of the organic moiety and high mechanical strength, good chemical resistance and high thermal stability of the inorganic component [1-3]. The properties of hybrid coatings can thus be designed by taking advantage of the fundamental different properties of these two components. Interesting applications for hybrid materials include wear and corrosion protection of metals, optics [4], primer solution [5], dental fillers [6], bone cement [7], water-repellent glass [8], transparent and abrasion-resistant coatings with fire-retardant properties and for prevention of wax deposition during transport in oil and gas pipelines [9]. Hybrid inorganic-organic coatings can also be used to modify and improve the surface properties of metals such as steel [10].

The sol-gel method is versatile and is applicable for synthesizing hybrid inorganic-organic coatings. The method is gentle in terms of a low temperature, and the coatings may be readily applied to most metallic substrates. Sol-gel silica systems are preferred because they may provide good hydrophilic wetting and good adhesion to the substrate surface [1]. Strong covalent bonds in the hybrid inorganic-organic material can be formed either by mixing organic components directly into the inorganic matrix in the sol-gel systems, taking advantage of the functional groups within the polymer which react with hydrolyzed inorganic precursors, or by utilizing alkoxysilanes as precursors wherein one or several alkoxy groups attached to the silicon are substituted by alkyl groups [10-13]. This approach can be applied for synthesizing sols for metal coatings, and for instance, Li et al. [14] coated aluminum with a triethoxysilane-based sol. The corrosion resistant behavior was improved during electrochemical/potentiodynamic polarization [14]. However, the most common use of substituted alkoxysilanes is as adhesion promoters between two different materials, and organofunctional silanes like 3-(aminopropyl)triethoxysilane (γ-APS) have been used to facilitate good bonding and to improve adhesion to organic coatings with any kind of substrate [15-17]. γ-APS based sols have been developed [18] and used as the basis for the preparation of wear resistant coatings by the addition of nanoparticles [19]. Coatings based on aminopropyl silane have currently been studied as barriers for preventing wax deposition [9]. The hybrid aminopropyl silane-based coatings showed good ability to reduce the thickness of the waxy layer which deposited compared to plain steel and commercial paints. Männle et al.

[18] developed a sol-gel synthesis route for γ-APS, but the properties of the γ-APS-based coatings have not previously been characterized.

In this work we demonstrate the feasibility of using hybrid aminopropyl silane-based sols for the preparation of coatings on steel substrates. Steel is commonly used for oil and gas pipelines, however, corrosion and wax deposition cause unwanted shut-downs due to maintenance. Thus the possibility of coatings the steel surfaces with γ-APS-based systems was explored. Generally, for tetraethoxysilane, the hydrolysis reaction is promoted at low pH. Due to this, it was desirable to investigate the feasibility of pH reduction in a relatively concentrated γ-APS in order to control the hydrolysis and condensation reactions. The coatings prepared by using different γ-APS-based sols have been characterized with respect to homogeneity, smoothness, thickness, wear resistance in addition to their wetting by water as well as an organic liquid.

2. Experimental

3-(Aminopropyl)triethoxysilane (γ-APS, Sigma-Aldrich, > 97 %) was mixed with 2,2,6,6-tetramethylpiperidine (Tmpp, Sigma-Aldrich, ≥ 99 %) and dissolved in approximately 50 % of the total amount of 1-propoxy-2-propanol (PnP, Sigma-Aldrich, 99 %) in argon atmosphere in a chemical cleanroom (ISO class 7). Deionized water of 15 MΩcm was used for hydrolyzing the sols. If required, water was adjusted to different pH values by addition of hydrochloric acid (HCl, VWR International, > 25 %). Water was then mixed with the remaining part of 1-propoxy-2-propanol and added dropwise to the γ-APS solution. The solution was subsequently magnetically stirred and heated to 80 °C (90 °C for the sols containing HCl as the reaction kinetics were slower) under reflux and kept at this temperature for 60 min. The solution was cooled under reflux. Three parameters were varied during the experiments in order to determine the impact of the sol chemistry on the final coating properties; water/silane ratio (R), solvent/silane ratio (S) and pH of water during the hydrolysis reaction, hereby denoted as hydrolysis pH. The compositions studied are included in the ternary diagram in Figure 1. The sols are referred to as h-xR-yS where h reflects that the sol is a hydrolyzed aminopropyl silane, x represents the water/silane ratio, R, and y denotes the solvent/silane ratio, S. An HCl-suffix is attached to the sols and coatings hydrolyzed with a water-HCl mixture, and these are denoted “acidic”, while the sols and coatings hydrolyzed with neutral hydrolysis water are termed “neutral”. Furthermore, the

water/silane ratio was either 1.6 (here defined as hypostoichiometric with respect to hydrolysis), 3 (here defined as stoichiometric with respect to hydrolysis) or 5 (here defined as hyperstoichiometric with respect to hydrolysis). A summary of the composition of the sols is provided in Table 1. The silane concentration was calculated as the amount of γ-APS present in the sol and is given as mol % silane.

Substrates of stainless steel (E. A. Smith Stål og Metall AS, AISI SS 304, thickness 0.5 mm, 3·5 cm²) were ground and polished to a mirror shine. The sols were aged at 4 °C for 24 to 48 h before they were applied to the substrates. Coating of the substrates was performed with a dip coater (KSV DCX2) in a clean room (ISO 7) in nitrogen atmosphere to avoid reactions between the basic amine groups and carbon dioxide from ambient air. The withdrawal speed was varied between 5 and 20 mm/min. The coatings were thermally cured in a chamber furnace (Carbolite HT/28CR) at 140 °C for 2 h with a subsequent hold at 160 °C for 3 h. The heating rate was 10 K/h from ambient temperature to 140 °C and 20 K/h the remaining temperature increase up to 160 °C. The cooling rate was 100 K/h. One part of the sol was gelled in a beaker and dried at ambient conditions. Subsequently, thermogravimetric analysis (TGA, Netzsch STA449C on 19 TASC 414/3) was conducted on the dried gels with a heating rate of 120 K/h.

A Micromeritics Tristar 3000 analyzer was used to measure the nitrogen adsorption and desorption isotherms of a selection of the hybrid aminopropyl silane-based gels at 77.3 K. The gels were dehydrated at 250 °C under vacuum prior to the analysis.

The viscosity of selected sols was measured at 5 °C under nitrogen atmosphere using a Haake Mars Modular Advanced Rheometer System (Thermo Scientific) with a cup cone geometry. The sols were stored at 5 °C for 4 months prior to the viscosity measurements.

^{29}Si NMR signals of a selection of the hybrid aminopropyl silane-based sols aged 24 h or 4 months at 5 °C were recorded with a Bruker Ultrashield 400 MHz Plus system equipped with a 5 mm PABBO-BB probe, operating at 79.495 MHz at 25 °C. Benzene d_6 in a coaxial insert capillary tube was used as an external reference.

The morphology of the hybrid aminopropyl silane-based coatings was assessed by atomic force microscopy (AFM) using a Nanosurf easyscan 2 Flex AFM (Nanoscience Instruments, ACL-A, TM cantilever tip) and Agilent Technologies 5500 AFM fitted with AC Mode III controller (Agilent Technologies, Veeco and Nanosensors (PPP-NHCR-20 with a nominal force constant of 42 N/m and radius < 10 nm) cantilever tips) in tapping mode. The AFM images were recorded by flattening the raw data using a third degree polynomial fit. AFM

was also used for surface roughness determination on an area of 10·10 μm². Roughness values are reported as the average roughness, $R_a = \frac{1}{n}\sum_{i=1}^{n}|z_i|$, where z_i is the measured topography at each x_i,y_i position.

Dry abrasion characterization of the coatings was carried out using a pin-on-disc tribometer (CSM Instruments TRN; S/N: 01-02668) with a silicon nitride (Si_3N_4) ball (6 $mm^{\varnothing}$), 0.5 N applied load with a linear speed of 0.5 cm/s. The resulting signal contained periodic noise, which was removed using a low pass fast Fourier transform filter. The thickness of the coatings was determined with stylus profilometry (Dektak 150, Veeco) by measuring the height difference at 4 different locations between the coating and the substrate as revealed by the abrasion track. Furthermore, scanning electron microscopy (Hitachi S-3400N) was used to acquire images of the resulting abrasion tracks by using secondary electron and backscatter electron detectors.

The surface wetting was studied by measuring the advancing contact angle by the sessile drop method using a goniometer-camera computer system (DSA100, Krüss, Germany). The contact angle at 25 °C was obtained between one layer of hydrolyzed aminopropyl silane on stainless steel and distilled water or pentadecane (Fluka, analytical standard). For a given system, the contact angle measurements were repeated three times and the reported values were corrected for surface roughness.

3. Results

3.1 Sol Characterization

The viscosity and shear stress as a function of shear rate are shown for selected sols in Figure 2 (a) and (b), respectively. The sols behaved as Newtonian liquids as the shear stress was linearly dependent on the shear rate. Figure 2 (c) presents the dependence of viscosity on the mol % silane in the sol. Increasing the solvent/silane ratio, S, reduced the viscosity, which was as expected simply from the effect of dilution. The viscosity generally increased with increasing silane concentration for a given R, and the effect on viscosity was more pronounced in the sols with higher R.

The distribution of structural entities of Si described as T^n species (defined in Scheme 1) for a selection of sols obtained by ^{29}Si NMR is presented in Figure 3 (a) and (b) for a reaction time of 24 h and 4 months, respectively. After 24 h, the hypostoichiometric sols contain T^1, T^2 and T^3 species whereas the stoichiometric and hyperstoichiometric sols have condensed to larger

T^2 and T^3 species. A prolonged reaction time of 4 months resulted in condensation of the sols to larger T^3 species. However, the stoichiometric and hyperstoichiometric sols were shown to have a larger fraction of T^2 in addition to the more condensed T^3 species compared to the hypostoichiometric sols with increasing R (Figure 3 (b)). A higher fraction of T^2 species indicated incompletely condensed Si-O-Si structures as is illustrated in Scheme 2 (a)-(c).

3.2 Coating Characterization

The thermal behavior of the coatings was assessed by thermogravimetry of dried gels from the hydrolyzed aminopropyl silane-based sols (featured in Figure S1). The hybrid materials were thermally stable up to approximately 350 °C. Furthermore, the gels (i.e. coatings) displayed a low surface area and a low pore volume. Moreover, nitrogen adsorption isotherms of selected silane-based gels are provided in Figure S2. The isotherms of the gels were characteristic of a non-porous solid (most probably a type 2 isotherm), which is typical for a non-porous silica gel [20]. Surface area measured by nitrogen adsorption was approximately 0.2 m^2/g and pore volume 10^{-4} cm^3/g confirming the low porosity.

Figures 4 (a) and (b) display the 2-D and 3-D AFM images of two acidic hybrid aminopropyl silane-based coatings. The corresponding neutral coatings are illustrated in Figure 4 (c) and (d). The coatings were generally smooth, homogeneous and crack-free.

The thickness as a function of R for the neutral and acidic coatings, respectively, is presented in Figure 5 (a) and (b). The thickness was shown to vary between 0.17 and 4.1 μm, and the thickness generally decreased with increasing R for a given S. The dependency of the thickness on the mol % silane is shown in Figure 5 (c) and (d) for the neutral and acidic coatings, respectively. The thickness increased with increasing mol % silane for a given R, and higher R resulted in thicker coatings for a given silane concentration. Furthermore, the thickness per mole of water added during hydrolysis was shown to increase linearly with the silane concentration as displayed in Figure 5 (e), and the acidic coatings were generally thinner than the neutral coatings. The thickness of the hybrid aminopropyl silane-based coatings increased with viscosity for a given R as displayed in Figure 5 (f). The thickness of the coatings is also provided in Table 2.

The observed contact angles of the acidic and neutral coatings with respect to water varied between 65 and 80 ° (Table 2). All coatings were wetted by liquid pentadecane.

SEM images of dry abrasion tracks of coatings with R= 5 and a variation in S are shown in Figure 6. The secondary electron (SE) SEM images (Figure 6 (a)) display the outline of the

wear track after 500 revolutions. The backscatter electron (BSE) image identifies dissimilarities in the chemical composition and is thus a useful tool for determining detachment of the coating from the steel surface. The magnified SE SEM images clearly show the lowest S coating to be completely delaminated in the abrasion track. The other two coatings seemed relatively intact, but displayed abrasion grooves in the direction of the abrasion. Figure 6 (b) shows the friction behavior of the coatings in Figure 6 (a) as a function of the number of revolutions of the Si_3N_4 ball on the coatings. A higher friction coefficient was measured for the coating with lowest S thus confirming the observations made SEM; a high friction coefficient signifies that the coating has flaked off and contact between the Si_3N_4 ball and the steel surface has been established. In this case one would thus expect delamination of the coating.

The effect of S on the abrasion resistance of the coatings is further elaborated for an acidic coating in Figure S3. For these coatings, the abrasion was limited, but the degree of delamination increased with increasing S as depicted in the magnified images in Figure S3 (b). In general, the acidic coatings have a higher abrasion resistance compared to the neutral coatings. For the neutral coatings, the abrasion resistance increased with decreasing coating thickness for a given R.

The effect of varying R at S=6, is shown in Figure S4 (a). The SEM images show similar tracks for all the coatings. Close-up of the abrasion tracks are displayed in Figure S4 (b), and it can be seen that parts of coatings h-3R-6S and h-5R-6S were delaminated. Ageing of coatings in ambient atmosphere up to two months showed no change in the abrasion resistance.

4. Discussion

The sol-gel method enables control of the final connectivity in the hybrid coatings by two reaction types, namely hydrolysis and condensation. By modifying the chemistry in order to promote one over the other, different microstructures and morphologies can be obtained. The hydrolysis and condensation reactions are outlined in Eq. 1-3 where R' is an alkyl group. Two different condensation reactions occur depending on the water/silane ratio, R. Low water/silane ratios result in alcohol producing condensation (Eq. 2, $R<1.5$), while higher ratios promote water producing condensation (Eq. 3, $R>1.5$).

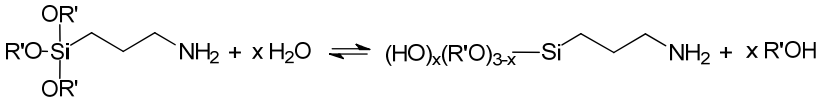

(1)

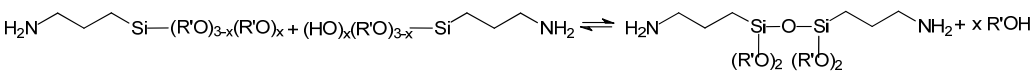

(2)

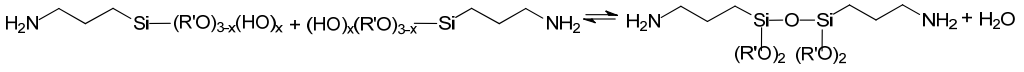

(3)

In the first step (Eq. 1), alkoxy groups are hydrolyzed, producing Si-OH which may further react with other Si-OH (or Si-OR') units and condense to form larger units or a network (T^1, T^2 and T^3 as shown in Scheme 1). Hydrolysis and condensation reactions occur simultaneously, but the reaction rates can be altered by varying the pH, reaction temperature, reaction time and the water/silane ratio, R [21]. Moreover, both the sol viscosity and the coating thickness were related to the silane concentration (Figures 2 and 5). By reducing the pH below 2 (the isoelectric point of silica) the hydrolysis reaction of tetraethoxy silane (TEOS) will dominate rendering the condensation rate slow [21], resulting in linear structures since the alkoxy groups can be fully hydrolyzed before condensation begins. For an aminopropyl silane, however, reducing the pH to the acidic region is not as easy because of the basic amine groups. Nevertheless, addition of HCl during the sol synthesis will reduce the pH enough to alter the chemistry in order to reduce the condensation reaction rate as was shown by the variation in the structural entities of the Si species as identified by ^{29}Si NMR in Figure 3. ^{29}Si NMR demonstrated that the rate of the condensation reaction was slower for the hypostoichiometric acidic and neutral sols evidenced by the presence of T^1 after 24 h whereas the neutral stoichiometric and hyperstoichiometric sols at the same reaction time already had condensed to T^2 and T^3 structural entities. The stoichiometric and hyperstoichiometric sols were shown to have a larger fraction of T^2 in addition to T^3 with increasing R which resulted in incompletely condensed cage structures as illustrated in Scheme 2. The high fraction of T^2 can also explain the higher viscosity which was observed for the aged hyperstoichiometric sol as these units would be connected in chains [22]. Analogously, sols constituting mainly T^3 species would be expected to have a cage-like structure made up of single T^3 entities (Scheme 2 (d)) as demonstrated by Cordes et al. [22], and a lower viscosity can be assumed for these sols compared to the chained sols.

The coatings were smooth as illustrated by the AFM images in Figure 4 with contact angles with water between 65 and 80 °. Due to the propyl groups, the coatings were also wetted by an organic liquid. We have previously studied the properties of similar γ-APS coatings in order to simulate wax deposition conditions from oil composed of a binary test fluid of

n-decane and n-tetracosane [9]. Compared to thicker, commercial paints, the γ-APS-based coatings were superior with respect to reduction of wax deposition, which could indicate that the obtained wetting properties are beneficial with respect to prevention of wax deposition. The dry abrasion resistance studies identified two types of behavior in the hybrid aminopropyl silane-based coatings; the coatings were either delaminated or smeared. Coating delamination was characterized by a higher friction coefficient with corresponding SEM images which displayed that the delaminated coatings had flaked off, while smearing was identified by a lubricating behavior. The abrasion resistance and degree of smearing of the acidic coatings decreased with increasing S. However, for the neutral coatings, increasing S (reducing coating thickness and silane concentration) improved the abrasion performance of the neutral coatings, and a smearing type behavior could then be observed. The smeared coatings were thinner than the delaminated coatings. The different behavior of the acidic and neutral coatings with respect to the degree of delamination was related to the chemical difference in the parent sols. In terms of chemistry, the degree of condensation into T^2 and T^3 entities could be modified by changing sol parameters such as reaction time, R and pH. The degree of condensation was reflected in the abrasion resistance of the coatings; a large fraction of T^3 entities in the sols aged 24 h resulted in delaminated coatings (hyperstoichiometric, R=5) whereas the presence of T^1 entities after 24 h (hypostoichiometric, R=1.6) provided coatings which smeared upon abrasion. Finally, whereas a delaminated coating is disrupted and thus will provide no further protection chemically nor mechanically, a smeared coating should still be able to chemically protect the steel surface to a certain extent as long as the coating is covering the whole surface.

5. Conclusion

Smooth and homogeneous hybrid inorganic-organic silica-based coatings were synthesized utilizing sol-gel chemistry with an aminopropyl silane as precursor at acidic or neutral hydrolyzing conditions. The inorganic part of the hybrid material increased the thermal stability of the coatings up to 350 °C. The hybrid aminopropyl silane-based coatings displayed a low pore volume and a low surface area. The coating thickness was in the range 0.17-4.1 μm with roughness in the nm range. The thickness and the roughness of the coatings could be tailored by optimizing the water/silane ratio in the sols. The coatings prepared at acidic hydrolysis conditions displayed better abrasion resistance than the coatings prepared at

neutral hydrolysis conditions. Delamination during abrasion was less pronounced in the coatings prepared at acidic hydrolysis conditions compared to coatings of similar thickness prepared at neutral hydrolysis conditions. The coatings were hydrophilic as demonstrated by water contact angles between 65 and 80 °. However, liquid pentadecane was also shown to wet the coatings.

Acknowledgements

This work was financially supported by The Research Council of Norway (grant no. 180038), Statoil, Total, BrederoShaw, Inpex, Tuboscope, Jotun, Carboline, 3M and AkzoNobel (Smoothpipe project).

The authors would also like to thank Monica Pilz and Sivakanesar Luxsacumar for their assistance and discussions with regards to the contact angle measurements. Huaitian Bu is acknowledged for the invaluable discussions regarding sol synthesis.

References

[1] F. Mammeri, E. Le Bourhis, L. Rozes and C. Sanchez, *J. Mater. Chem.*, 2005, 15, 3787.

[2] J. D. Mackenzie, Q. Huang and T. Iwamoto, *J. Sol-Gel Sci. Technol.*, 1996, 7, 151.

[3] G. L. Wilkes, H.-H. Huang, R. H. Glaser, *Adv. Chem, Ser.*, 1990, 224, 207.

[4] C. Sanchez, F. Ribot, L. Rozes and B. Alonso, *Mol. Cryst. and Liq. Cryst.*, 2000, 354, 143.

[5] J. Wen, V. J. Vasudevan and G. L. Wilkes, *J. Sol-Gel Sci. Technol.*, 1995, 5, 115.

[6] Y. Wei, D. Jin, G. Wei, D. Yang and J. Xu, *J. Appl. Polym. Sci.*, 1998, 70, 1689.

[7] J.-M. Yang, C.-S. Lu, Y.-G. Hsu and C.-H. Shih, *J. Biomed. Mater. Res. (Appl. Biomater.)*, 1997, 28, 143.

[8] M. A. Aegerter, R. Almeida, A. Soutar, K. Tadanaga, H. Yang and T. Watanabe, *J. Sol-Gel Sci. Technol.*, 2008, 47, 203.

[9] S. G. Johnsen, S. M. Hanetho, P. Tetlie, S. T. Johansen, M.-A. Einarsrud, I. Kaus, C. R. Simon. Paraffin Wax Deposition Studies on Coated and Non-coated Steel Surfaces. Heat Exchanger Fouling and Cleaning IX - 2011, Crete, Greece, June 06 - June 10.

[10] D. Wang and G. P. Bierwagen, *Prog. Org. Coat.*, 2009, 64, 327.

[11] C. Sanchez, L. Rozes, F. Ribot, C. Laberty-Robert, D. Grosso, C. Sassoye, C. Boissiere and B. M. Novak, *Adv. Mater.*, 1993, 5, 422.

[12] P. Judeinstein and C. Sanchez, *J. Mater. Chem.*, 1996, 6, 511.

[13] J. Wen and G. L. Wilkes, *Chem. Mater.*, 1996, 8, 1667.

[14] Y.-S. Li and A. Ba, *Spectrochim. Acta, Part A,* 2008, 70, 1013.

[15] E. T. Vandenberg, L. Bertilsson, B. Liedberg, K. Udval, R. Erlandsson, H. Elwing and I. Lundström, *J. Colloid Interface Sci.*, 1991, 147, 103.

[16] S. Naviroj, S. R. Culler, J. L. Koenig and H. Ishida, *J. Colloid Interface Sci.*, 1984, 97, 308.

[17] S. R. Culler, H. Ishida and J. L. Koenig, *Polym. Compos.*, 1986, 7, 231.

[18] F. Männle, C. Simon, J. Beylich, K. Redford, B. Sommer, E. Hinrichsen, E. Andreassen, K. Olafsen and T. Didriksen, 2005, *WO2005100450*.

[19] C. Simon and F. Männle, *Paint Coatings Ind.*, 2005, 21, 104.

[20] P. C. Hiemenz and R. Rajagopalan, Principles of Colloid and Surface Chemistry, CRC press, Boca Raton, FL, USA, 1997.

[21] C. J. Brinker and G. W. Scherer, Sol-Gel Science: The Physics and Chemistry of Sol-Gel Processing. Academic Press, Inc., San Diego, 1990.

[22] D. B. Cordes, P. D. Lickiss and F. Rataboul, *Chem. Rev.*, 110, 2010, 2081.

[23] M.-C. B. Salon and M. N. Belgacem, *Colloids Surf., A.*, 366, 2010, 147.

Tables

Table 1: Amount of precursors used for the preparation of the different hydrolyzed aminopropyl silane-based sols, water/silane ratio (R), solvent/silane ratio (S) and pH of the distilled water used during the hydrolysis reaction.

Sol	Precursors (mol)		mol % silane	$R = \frac{n_{H_2O}}{n_{Si}}$	$S = \frac{n_{solvent}}{n_{Si}}$	Hydrolysis pH
	γ-APS	Tmpp				
h-1.6R-0.6S	0.4338	0.002152	31.2	1.6	0.6	6.2
h-1.6R-3S	0.1084	0.0005381	17.8	1.6	3	6.2
h-1.6R-6S	0.1084	0.0005381	11.6	1.6	6	6.2
h-3R-0.6S	0.4338	0.002152	21.7	3	0.6	6.2
h-3R-3S	0.4338	0.002152	14.3	3	3	6.2
h-3R-6S	0.4338	0.002152	10.0	3	6	6.2
h-5R-0.6S	0.4338	0.002152	15.1	5	0.6	6.2
h-5R-3S	0.4338	0.002152	11.1	5	3	6.2
h-5R-6S	0.4338	0.002152	8.3	5	6	6.2
h-1.6R-0.6S-HCl	0.2169	0.001097	31.2	1.6	0.6	0.8
h-1.6R-3S-HCl	0.4338	0.002152	17.8	1.6	3	0.8
h-1.6R-6S-HCl	0.4338	0.002152	11.6	1.6	6	0.8
h-3R-0.6S-HCl	0.4338	0.002152	21.7	3	0.6	0.8
h-3R-3S-HCl	0.07229	0.0003587	14.3	3	3	0.8
h-3R-6S-HCl	0.4338	0.002152	10.0	3	6	0.8

Table 2: Thickness, average surface roughness (Ra) and contact angle for the synthesized hydrolyzed aminopropyl silane-based coatings.

Coating	Thickness (μm)	R_a (nm)	Water contact angle, °
h-1.6R-0.6S	4.0 ± 0.09	0.67	79 ± 2.0
h-1.6R-3S	1.4 ± 0.06	9.3	72
h-1.6R-6S	0.35 ± 0.05	0.60	72 ± 1.5
h-3R-0.6S	2.9 ± 0.4	0.60	76 ± 2.5
h-3R-3S	0.98 ± 0.02	1.1	79 ± 3.6
h-3R-6S	0.32 ± 0.002	1.0	76 ± 1.1
h-5R-0.6S	2.0 ± 0.05	0.21	67 ± 4.1
h-5R-3S	0.66 ± 0.06	0.39	72 ± 0.8
h-5R-6S	0.26 ± 0.02	0.36	74 ± 3.0
h-1.6R-0.6S-HCl	4.1 ± 0.6	0.31	65 ± 2.0
h-1.6R-3S-HCl	0.4 ± 0.02	5.5	71 ± 2.0
h-1.6R-6S-HCl	0.17 ± 0.05	0.60	69 ± 3.2
h-3R-0.6S-HCl	2.4 ± 0.3	0.44	73 ± 4.1
h-3R-3S-HCl	1.0 ± 0.07	0.57	76 ± 2.1
h-3R-6S-HCl	0.32 ± 0.004	0.51	72 ± 1.7

Figure captions

Figure 1. Composition of the different hybrid aminopropyl silane-based sols.

Figure 2. (a) Viscosity and (b) shear stress as a function of the applied shear rate for a selection of hybrid aminopropyl silane-based sols. (c) Viscosity as a function of the silane concentration for the sols in (a) and (b).

Figure 3. Distribution of T^n species in a selection of the hybrid aminopropyl silane-based sols as measured by ^{29}Si NMR. (a) relates to sols aged 24 h ahile (b) represents sols aged 4 months.

Figure 4. 2D and 3D AFM images displaying the surface of the acidic (a) and neutral (c) hybrid aminopropyl silane-based coatings. The images of the corresponding surface roughness in (b) and (d) have been smoothed using a second degree polynomial fit.

Figure 5. Thickness of neutral (a and c) and acidic (b and d) coatings with respect to water/silane ratio, R, and mol % silane. Thickness per mole water as a function of mol % silane, (e), and as a function of sol viscosity, (f).

Figure 6. (a) SEM images (SE and BSE) of the resulting abrasion tracks of hybrid aminopropyl silane-based coatings with R=5, and varying S from 0.6 to 6 and linear speed 0.5 cm/s after 500 revolutions. Images of higher resolution is also shown for the SE images. (b) Friction coefficient response of the coatings in (a). The friction coefficient of uncoated polished stainless steel is included for comparison.

Scheme 1: The different T^n species that may form during the reaction between water and a trialkoxysilane, modified from [23]. R denotes an alkyl group whereas OR' is an alkoxy group.

Scheme 2: (a) Ladder, (b) linear and (c) partial cage structures giving rise to the different condensed (T^1, T^2 and T^3) signals in the ^{29}Si NMR spectra. A fully condensed T^3 structure, which in this case is in the form of γ-APS, is displayed in (d).

Figures

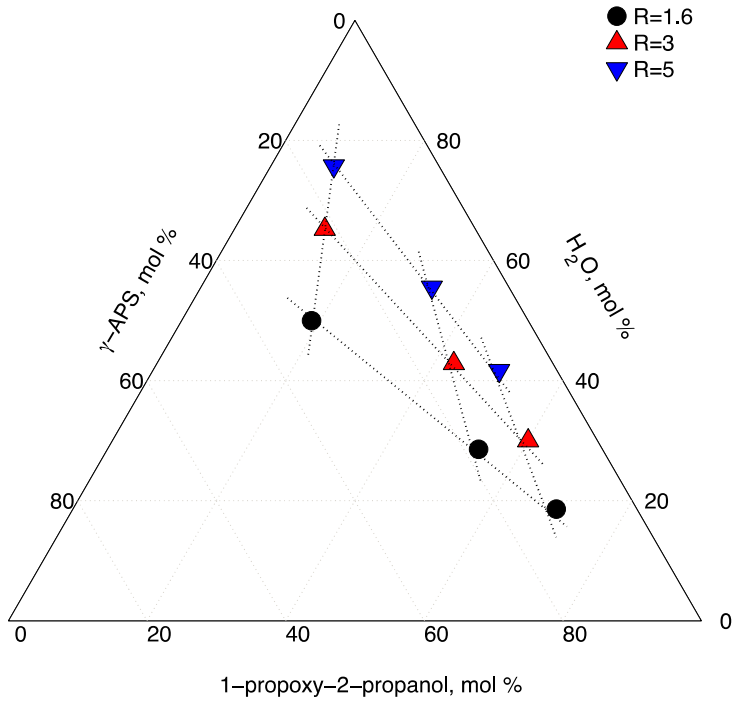

Figure 1. Composition of the different hybrid aminopropyl silane-based sols.

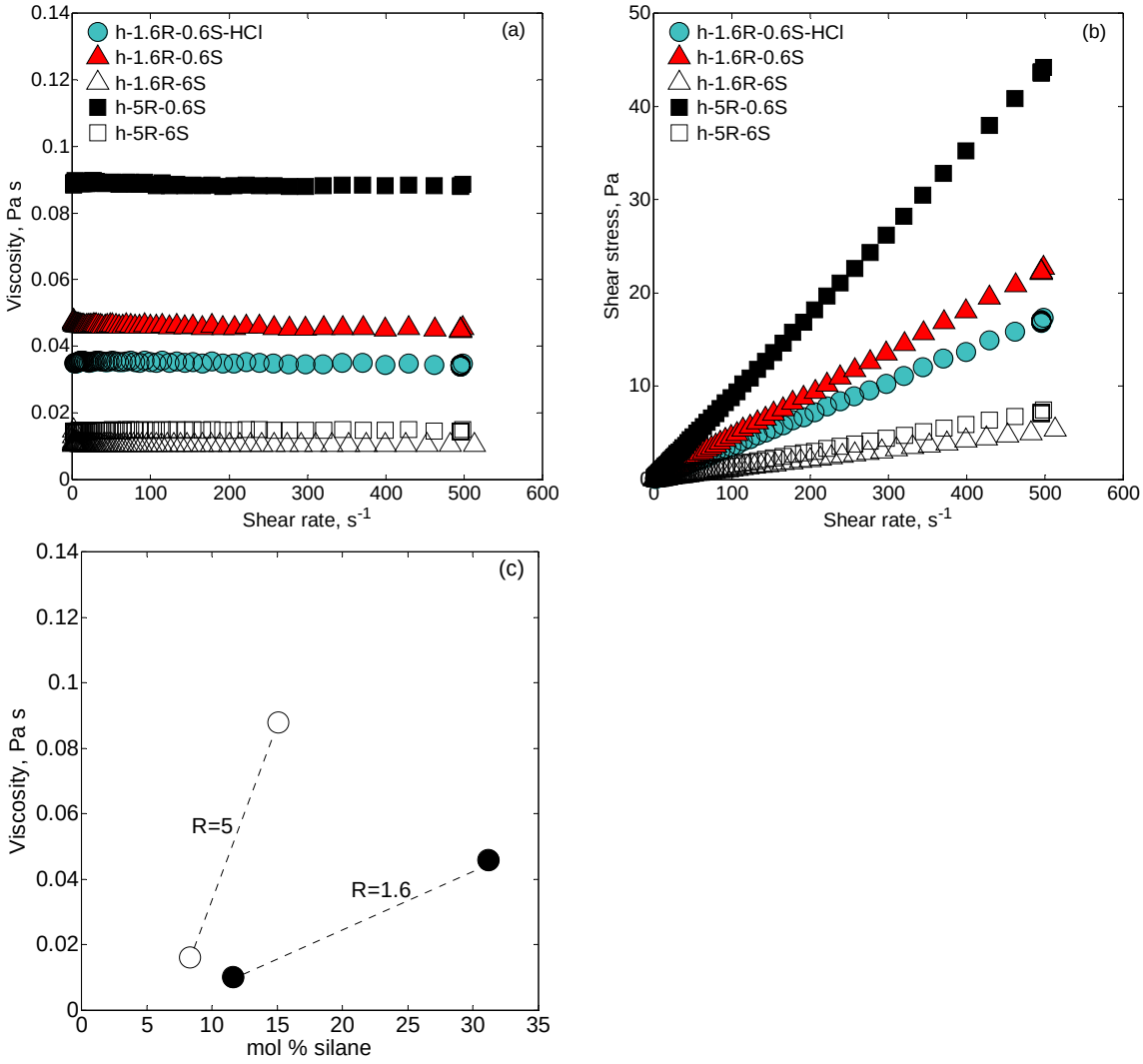

Figure 2. (a) Viscosity and (b) shear stress as a function of the applied shear rate for a selection of hybrid aminopropyl silane-based sols. (c) Viscosity as a function of the silane concentration for the sols in (a) and (b).

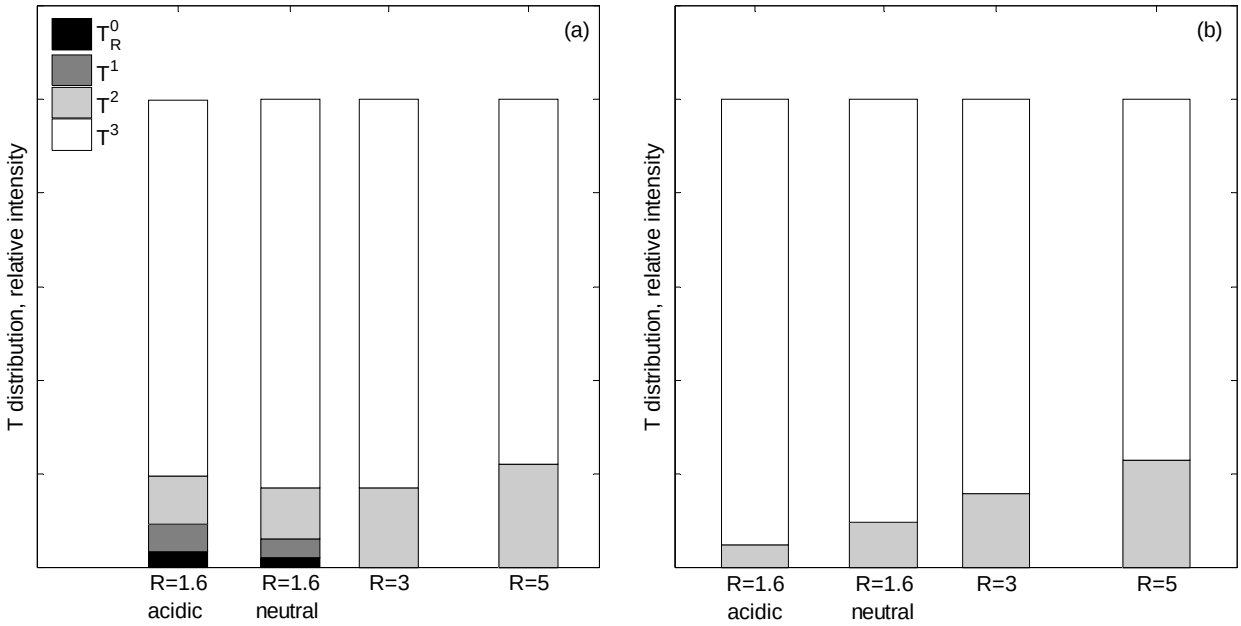

Figure 3. Distribution of T^n species in a selection of the hybrid aminopropyl silane-based sols as measured by ^{29}Si NMR. (a) relates to sols aged for 24 h while (b) represents sols aged for 4 months.

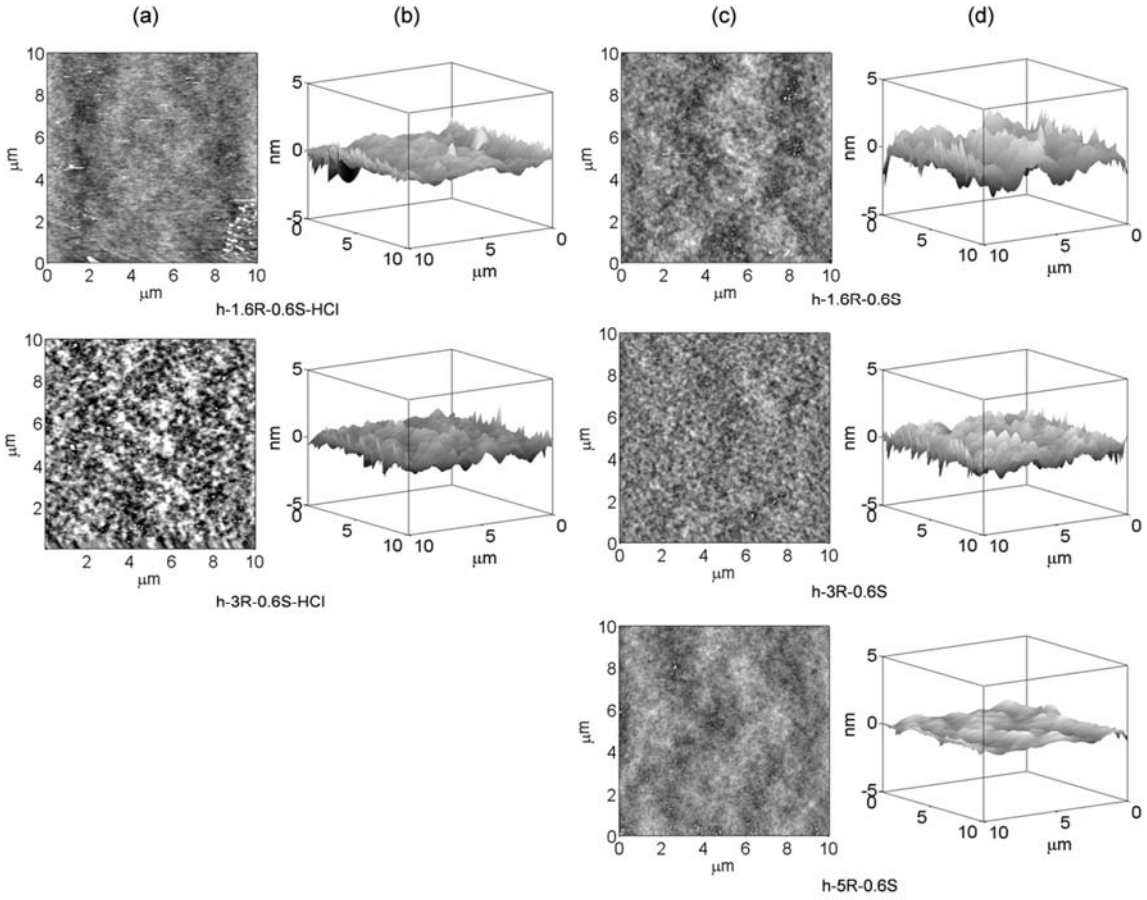

Figure 4. 2D and 3D AFM images displaying the surface of the acidic (a) and neutral (c) hybrid aminopropyl silane-based coatings. The images of the corresponding surface roughness in (b) and (d) have been smoothed using a second degree polynomial fit.

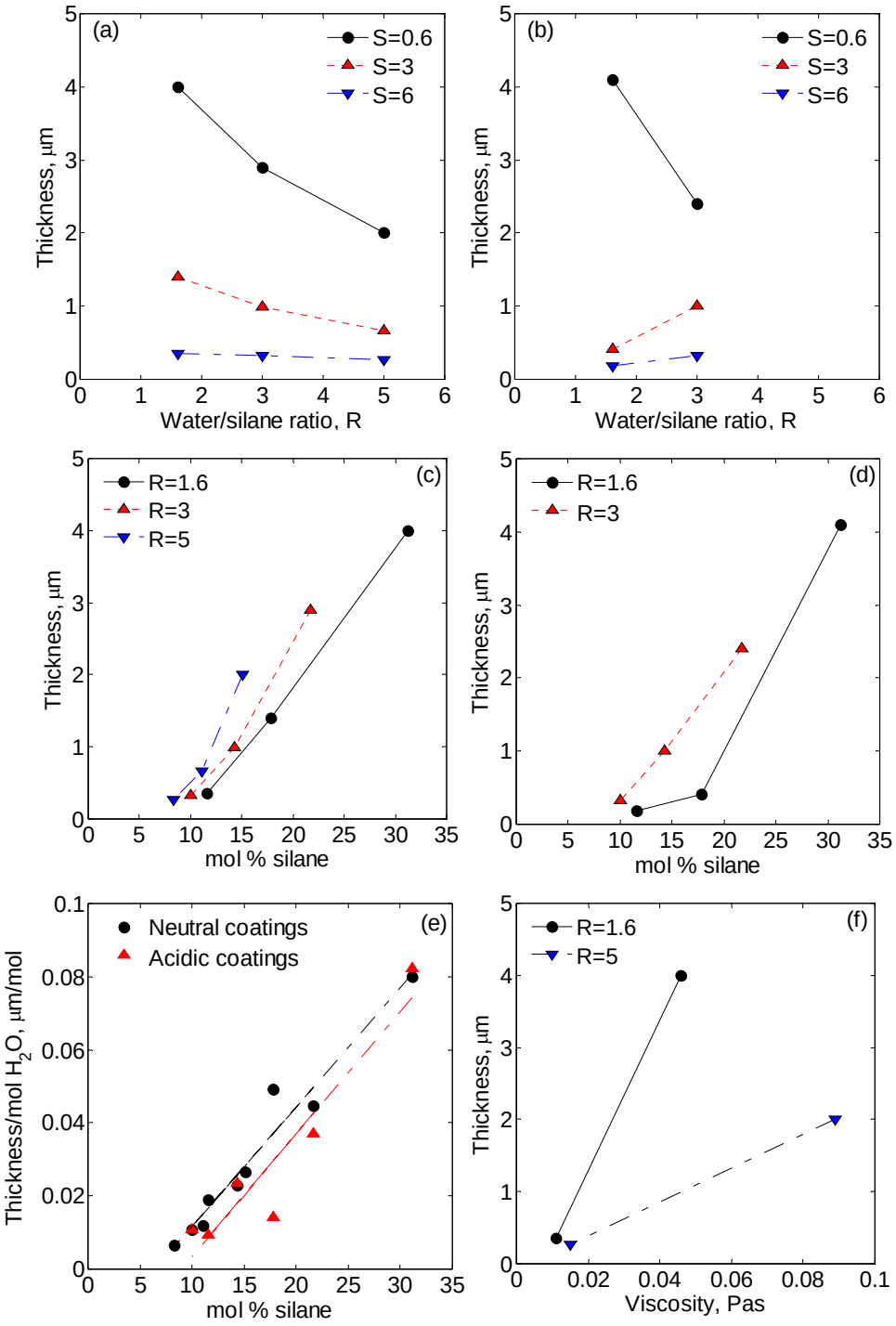

Figure 5. Thickness of neutral (a and c) and acidic (b and d) coatings with respect to water/silane ratio, R, and mol % silane. Thickness per mole water as a function of mol % silane, (e), and as a function of sol viscosity, (f).

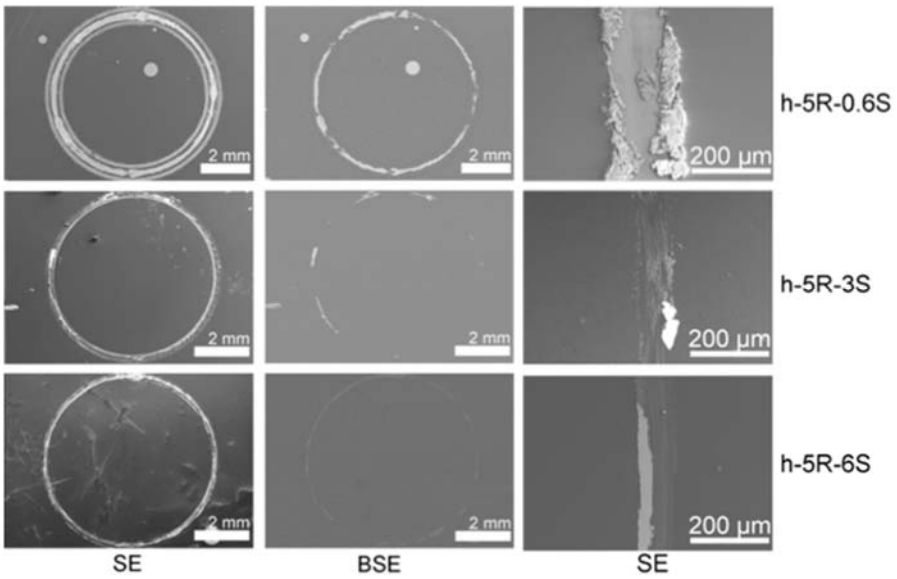

(a)

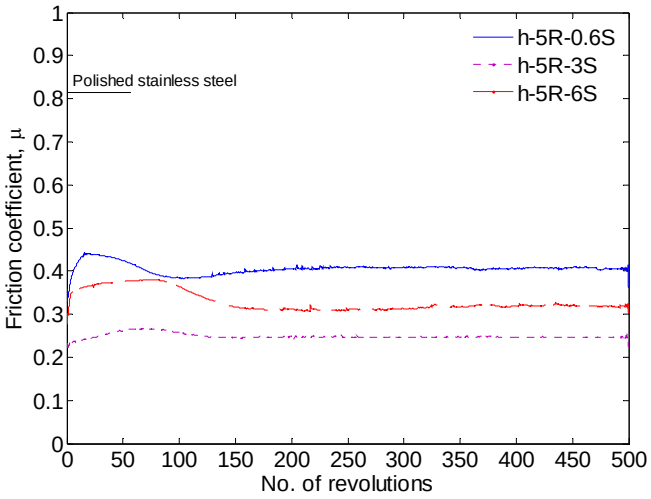

(b)

Figure 6 Abrasion tracks of hybrid aminopropyl silane-based coatings with water/silane ratio, R=5, and varying solvent/silane ratio, S, from 0.6 to 6 and linear speed 0.5 cm/s. (a) SEM images (SE and BSE) of the resulting wear track after the completion of 500 revolutions. Images of higher resolution is also shown for the SE images. (b) Friction coefficient response of the coatings in (a). The friction coefficient of uncoated polished stainless steel is included for comparison.

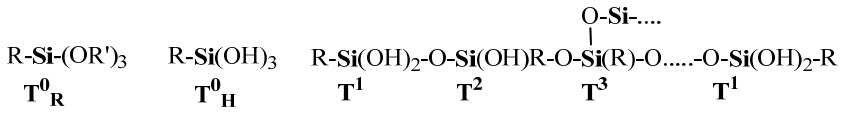

Scheme 1: The different T^n species that may form during the reaction between water and a trialkoxysilane, modified from [23]. R denotes an alkyl group whereas OR' is an alkoxy group.

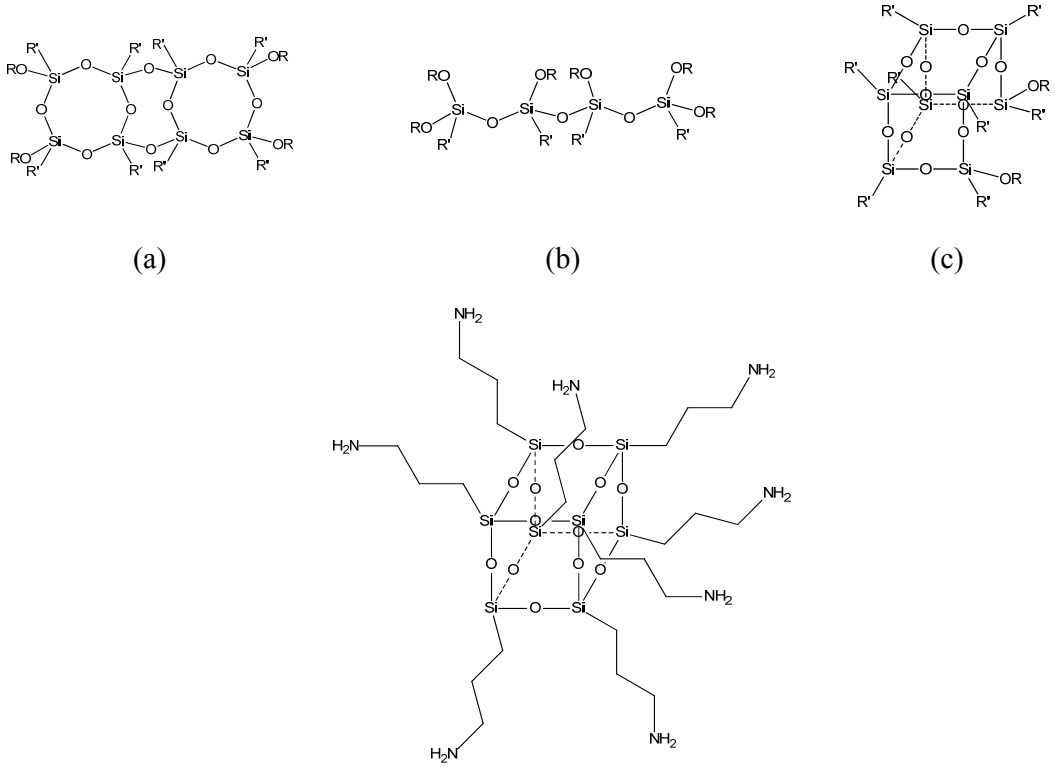

Scheme 2: (a) Ladder, (b) linear and (c) partial cage structures giving rise to the different condensed (T^1, T^2 and T^3) signals in the ^{29}Si NMR spectra. A fully condensed T^3 structure, which in this case is in the form of γ-APS, is displayed in (d).